

# Journal of Visualized Experiments

## Versatile dual-inlet sample introduction system for multi-mode single particle inductively coupled plasma mass spectrometry analysis and validation --Manuscript Draft--

<b>Article Type:</b>	Invited Methods Article - JoVE Produced Video
<b>Manuscript Number:</b>	JoVE61653R2
<b>Full Title:</b>	Versatile dual-inlet sample introduction system for multi-mode single particle inductively coupled plasma mass spectrometry analysis and validation
<b>Section/Category:</b>	JoVE Chemistry
<b>Keywords:</b>	Inductively coupled plasma mass spectrometry; nanoparticles; micro droplet; dual-inlet system; multi-mode quantification; validation
<b>Corresponding Author:</b>	Fabian Kriegel Bundesinstitut fur Risikobewertung Berlin, Berlin GERMANY
<b>Corresponding Author's Institution:</b>	Bundesinstitut fur Risikobewertung
<b>Corresponding Author E-Mail:</b>	Fabian.Kriegel@bfr.bund.de
<b>Order of Authors:</b>	Daniel Rosenkranz Fabian L. Kriegel Emmanouil Mavrakis Spiros A. Pergantis Philipp Reichardt Jutta Tentschert Norbert Jakubowski Peter Laux Ulrich Panne Andreas Luch
<b>Additional Information:</b>	
<b>Question</b>	<b>Response</b>
Please indicate whether this article will be Standard Access or Open Access.	Open Access (US\$4,200)
Please indicate the <b>city, state/province, and country</b> where this article will be <b>filmed</b> . Please do not use abbreviations.	Berlin, Deutschland

Bundesinstitut für Risikobewertung (BfR) • Postfach 12 69 42 • D - 10609 Berlin

 German Federal Institute for Risk Assessment (BfR)  
 Max-Dohrn-Strasse 8-10  
 10589 Berlin  
 www.bfr.bund.de

**To:**  
**Editor-in-Chief of the Journal**  
**“Journal of Visualized Experiments”**

 Andreas Luch, MD, PhD  
 Professor of Pharmacology & Toxicology  
 Freie Universität Berlin  
 Department Head  
 Chemical and Product Safety@BfR

Ihre Zeichen und Nachrichten vom	Gesch.-Z.: Bitte bei Antwort angeben	Tel.-Durchwahl/Fax 49-30-18412-27513	Datum 2020 – 05 – 14	Org.-Einheit/Ansprechpartner 7/ Rosenkranz, Kriegel, Luch
----------------------------------	--------------------------------------	---	-------------------------	--

Dear Editor,

On behalf of all authors we would like to submit the following manuscript for publication in the journal *Journal of Visualized Experiments*:

**“Improved dual-inlet system for robust multi-mode single particle ICP-MS validation”**

Standards and reference substances ensure reliable identification and quantification in mass spectrometry based systems. Yet, in the field of nanoparticle size characterization with the help of single particle inductively coupled plasma mass spectrometry (sp-ICP-MS) such standards are only available for a few elements such as gold or silver. The reason for this shortage is the technical challenge of producing stable standards with a narrow particle size distribution. The application of standards that differ in physicochemical properties from the actual particles to be analyzed, however, results in the measurement of incorrect particle sizes and loss of information. Precise nanoparticle characterization is essential for applied sciences such as nanomedicine or nanoengineering though.

Due to the importance of nanotechnology and the associated consequences for its further development, we searched for a solution to overcome this problematic lack of standards. Instead of synthesizing new and improved standards of further elements, we found a novel and creative solution that will help researchers to characterize nanoparticle size distributions in an easy, robust and extremely sensitive manner without relying on any standard.

By using a microdroplet generator (MDG) as sample introduction system coupled online to an ICP-MS device, we were able to eliminate the need for a size reference standard in sp-ICP-MS. We have tested this setup with three different particle types to demonstrate the applicability of our approach. Other state-of-the-art techniques were carried out in comparison. In addition, a cross calibration has been performed with ionic solutions utilizing the MDG and a conventional pneumatic nebulizer. By

application of our methodology the occurrence of split events could be significantly reduced and the sensitivity of the system greatly enhanced. In our manuscript we further introduce a new evaluation method for the sp-ICP-MS data collected.

We think that our report on the development of a novel and standard independent sp-ICP-MS sample introduction system in combination with its superior sensitivity would perfectly fit the ambition and scope of your renowned journal. Therefore we hope that our work might be of interest for you and the readership of the *Journal of Visualized Experiments*.

All authors and our institution agree to the submission of this paper. We agree with the journal's policies and requirements and declare no conflicts of interest.

We are very much looking forward to hearing from you at your earliest convenience.

On behalf of all co-authors,

Sincerely yours,

*Daniel Rosenkranz, M.Sc., Ph.D. candidate*

*Fabian Kriegel, M.Sc., Ph.D. candidate*

*Andreas Luch, M.D., Ph.D.*

**TITLE:**

Versatile Dual-Inlet Sample Introduction System for Multi-Mode Single Particle Inductively Coupled Plasma Mass Spectrometry Analysis and Validation

**AUTHORS AND AFFILIATIONS:**

Daniel Rosenkranz<sup>1,\*</sup>, Fabian L. Kriegel<sup>1</sup>, Emmanouil Mavrakis<sup>2</sup>, Spiros A. Pergantis<sup>2</sup>, Philipp Reichardt<sup>1</sup>, Jutta Tentschert<sup>1</sup>, Norbert Jakubowski<sup>4</sup>, Peter Laux<sup>1</sup>, Ulrich Panne<sup>3</sup>, Andreas Luch<sup>1</sup>

<sup>1</sup>German Federal Institute for Risk Assessment (BfR), Department of Chemical and Product Safety, Max-Dohrn-Strasse, Berlin, Germany

<sup>2</sup>Environmental Chemical Processes Laboratory, Department of Chemistry, University of Crete, Voutes Campus, Heraklion, Greece

<sup>3</sup>Federal Institute for Materials Research and Testing (BAM), Richard-Willstätter-Strasse, Berlin, Germany

<sup>4</sup>SPETEC GmbH, Am Kletthamer Feld, Erding, Germany

Corresponding author:

Fabian Kriegel (fabian.kriegel@bfr.bund.de)

E-mail address of co-authors:

Daniel Rosenkranz (daniel.rosenkranz@bfr.bund.de)

Emmanouil Mavrakis (mavrmanos@gmail.com)

Spiros A. Pergantis (spergantis@uoc.gr)

Philipp Reichardt (philipp.reichardt@bfr.bund.de)

Jutta Tentschert (jutta.tentschert@bfr.bund.de)

Norbert Jakubowski (norbert.jakubowski@spetec.de)

Peter Laux (peter.laux@bfr.bund.de)

Ulrich Panne (ulrich.panne@bam.de)

Andreas Luch (andreas.luch@bfr.bund.de)

**KEYWORDS:**

inductively coupled plasma mass spectrometry, nanoparticles, micro droplet, dual-inlet system, multi-mode quantification, validation

**SUMMARY:**

Here we provide a protocol for the use of a dual-inlet system for single particle inductively coupled mass spectrometry which allows for a standard independent nanoparticle characterization.

**ABSTRACT:**

Metal-containing nanoparticles (NP) can be characterized with inductively coupled plasma mass spectrometers (ICP-MS) in terms of their size and number concentration by using the single-particle mode of the instrument (spICP-MS). The accuracy of measurement depends on the setup, operational conditions of the instrument and specific parameters that are set by the

user. The transport efficiency of the ICP-MS is crucial for the quantification of the NP and usually requires a reference material with homogenous size distribution and a known particle number concentration.

Currently, NP reference materials are available for only a few metals and in limited sizes. If particles are characterized without a reference standard, the results of both size and particle number may be biased. Therefore, a dual-inlet setup for characterizing nanoparticles with spICP-MS was developed to overcome this problem. This setup is based on a conventional introduction system consisting of a pneumatic nebulizer (PN) for nanoparticle solutions and a microdroplet generator ( $\mu$ DG) for ionic calibration solutions. A new and flexible interface was developed to facilitate the coupling of  $\mu$ DG, PN and the ICP-MS system. The interface consists of available laboratory components and allows for the calibration, nanoparticle (NP) characterization and cleaning of the arrangement, while the ICP-MS instrument is still running.

Three independent analysis modes are available for determining particle size and number concentration. Each mode is based on a different calibration principle. While mode I (counting) and mode III ( $\mu$ DG) are known from the literature, mode II (sensitivity), is used to determine the transport efficiency by inorganic ionic standard solutions only. It is independent of NP reference materials. The  $\mu$ DG based inlet system described here guarantees superior analyte sensitivities and, therefore, lower detection limits (LOD). The size dependent LODs achieved are less than 15 nm for all NP (Au, Ag, CeO<sub>2</sub>) investigated.

## INTRODUCTION:

Inductively coupled plasma mass spectrometers are extensively used to quantify size and number of NP in various samples and matrices in the so called single particle mode<sup>1-3</sup>. The single particle mode is an operation of the data acquisition system with a short integration or dwell time. Each NP measured produces an integrated signal in this time interval (event measured in counts per second: cps) if an adequate dilution of the NP suspension was used to avoid double events. Calibration standard, as well as the sample, are usually introduced into the ICP-MS via a conventional sample introduction system based on pneumatic nebulization (PN)<sup>4</sup>. However, as a prerequisite, the sample introduction flow rate and transport efficiency ( $\eta$ ) must be determined to accurately quantify the metal mass per NP and to determine their number concentration in the suspension. The transport efficiency describes the ratio of the mass or particle number injected to the mass (waste collecting method) or particle number (counting method) detected by the ICP-MS<sup>5</sup>. The transport efficiency is most frequently determined using nanoparticle-based reference materials<sup>5</sup>. However, transport properties depend on the structure of the NP, and involves properties like composition and sample dispersant. Other influencing factors are instrumental parameters, like sample uptake rate, nebulizer gas flow rate, dwell time and total measurement time.

Since only limited nanoparticulate reference materials are available, the obtained NP analysis results can be biased due to differences in elemental composition between reference and sample particles. Besides the availability of a limited range of reference materials, the detection of multiple particle events per detector dwell time represents a further challenge. This may also

89 affect the accuracy of the transport efficiency to be determined.

90  
91 To be independent of reference materials, ideally, a sample introduction system with a  
92 transport efficiency of almost 100% is preferable. At the same time when a low volume is used  
93 compared to conventional introduction systems, higher particle number concentrations can be  
94 used. Even if two particles are close to each other both can be separately detected with the  
95  $\mu$ DG based system.

96  
97 The  $\mu$ DG is able to generate monodisperse droplets with a fixed volume in the pL range and is  
98 well-suited for this purpose<sup>6-9</sup>. The  $\mu$ DG facilitates the injection of both ionic and particulate  
99 samples in different solvents into the ICP-MS. In case of ionic metal samples, it is assumed that  
100 the droplets generated are fully desolvated on the way to the ICP. Accordingly, the droplet  
101 loses all water and a particle is formed from the remaining salt. The diameter of this particle is  
102 directly proportional to the concentration used. Thus, homemade reference standards of the  
103 same matrix, mass, and size, with varying concentration of the ionic solution of the NP to be  
104 investigated, can be produced in-house. The volume of a droplet can be calculated easily based  
105 on the droplet diameter measured by the  $\mu$ DG. This is not possible with a PN which produces a  
106 wide distribution of droplets with different diameters<sup>10,11</sup>. Due to the uniform sample  
107 introduction at high transport efficiency of 100% of the  $\mu$ DG, high instrument-specific analyte  
108 sensitivity can be achieved. Depending on the matrix used, this leads to lower limits of  
109 detection (LOD) of particle mass and size when compared to the results of conventional  
110 introduction systems based on PN<sup>12</sup>. However, due to the design of the  $\mu$ DG, samples cannot be  
111 exchanged easily when the ICP-MS system is still operating. Between measurements of  
112 different samples, the  $\mu$ DG has to be cleaned and afterwards flushed with the sample solution  
113 for system stabilization. In addition, its tolerance to heavy matrix samples has not been tested  
114 to great extent. Moreover, due to the extremely low flow rates, the analysis time to achieve  
115 good statistics would be extremely long, which limits its practical use, if “real” samples, as for  
116 instance environmental waters, should be analyzed.

117  
118 To overcome these limitations, the  $\mu$ DG has been previously operated in combination with a  
119 conventional pneumatic nebulizer based system, which was given the name of a dual inlet  
120 system<sup>13</sup>. By introducing the calibration standards with the  $\mu$ DG and the NP suspension via a  
121 pneumatic nebulizer into the ICP-MS, Ramkorun-Schmidt et al. were able to take advantage of  
122 both systems<sup>13</sup>. Highly accurate determination of the metal mass fraction of Au and Ag NP were  
123 achieved, without a need for transport efficiency determination. However, no particle number  
124 concentrations were determined with this dual inlet system. Also, cleaning and alignment of  
125 the  $\mu$ DG system was complicating the applicability for routine analysis.

126  
127 In this paper, we propose a flexible dual inlet interface for determining NP particle size and  
128 particle number concentration and demonstrate the assembly and practical use of it. Like the  
129 system of Ramkorun-Schmidt et al. it consists of both an  $\mu$ DG as well as PN sample introduction  
130 system. We demonstrate that the dual-inlet system, in its present stage of development, allows  
131 the application of three independent modes of analysis to investigate and characterize metal-  
132 containing NPs. Our dual-inlet system simplifies the calibration procedure for NP determination

and improves the analytical figures of merit in particular the accuracy<sup>14</sup>. The inlet systems allow convenient sample exchange and cleaning of the  $\mu$ DG even when the ICP-MS is still operating, thereby reducing the overall analysis time and the risk of misalignment. In order to test the system performance well characterized reference NP (60 nm AuNP – NIST 8013, 75 nm AgNP – NIST 8017) are used for method validation and comparability.

## PROTOCOL:

### 1. Assembly of the dual-inlet sample introduction setup

NOTE: Details about different parts are shown in **Table 1**.

(Place **Table 1** here).

#### 1.1. Construction of a T-piece connector unit (**Figure 1 Part 1**).

NOTE: This part connects the conventional sample introduction system (step 1.2) and the  $\mu$ DG transport unit (step 1.3).

1.1.1. Insert a male and female ball joints to the opposite openings of a T-piece connector.

1.1.2. Secure the male and female ball joints by using a glass to metal adhesive (e.g., silicon glue).

1.1.3. Connect the female ball joint to the injector of the ICP-MS using a clamp.

#### 1.2. Attachment of a conventional sample introduction system (**Figure 1 Part 2**)

NOTE: This part is connected to the T-piece connector unit (step 1.1)

1.2.1. Combine an ICP-MS spray chamber with a pneumatic nebulizer (PN), which fits into the spray chamber being used.

1.2.2. Use a clamp to connect the spray chamber outlet to the male ball joint of the T-piece connector (described in step 1.1).

NOTE: The spray chamber outlet is usually equipped with a female ball joint connector. The combination shown in **Figure 1** consists of a nebulizer and an impact bead spray chamber. Instead of the impact bead spray chamber other spray chambers with transport efficiencies in range of 2 to 10% or higher can be used.

#### 1.3. Construction of the microdroplet transport unit (**Figure 1 Part 3**)

NOTE: This part connects the T-piece connector unit (step 1.1) and the  $\mu$ DG unit (step 1.4).

177  
178 1.3.1. Attach a demountable quartz torch, with its injector tube removed, to a laboratory stand  
179 with the torch inlet on the top using appropriate clamps.

180  
181 1.3.2. Block the torch plasma/auxiliary gas inlet by closed end gas connectors.

182  
183 NOTE: The sample is transported using a peristaltic pump to the nebulizer. Argon gas is used for  
184 sample nebulization into the spray chamber and further transportation into the plasma.

185  
186 1.3.3. Connect a helium gas line to the torch via its cooling gas inlet by using an appropriate gas  
187 connector.

188  
189 NOTE: The applied helium gas is used for the desolvation of generated droplets and act as a  
190 sheath gas preventing the droplet from a collision with the walls of the setup and in preventing  
191 the ICP-MS instrument from atmospheric oxygen insertion while the sample inlet head of the  
192  $\mu$ DG has to be removed for cleaning and sample exchange.

193  
194 1.3.4 Connect a 30 cm long conductive and flexible silicone tube (i.d. 0.75 cm), using an  
195 adapter, to the exit end of the torch (bottom of torch).

196  
197 1.3.5 Connect the downward end of the silicone tubing to the T-piece connector unit by  
198 stretching the flexible silicone tubing over its remaining vertical metal connection.

199  
200 NOTE: The flexible silicone tubing allows x-y-z tuning of the ICP-MS instrument with the  
201 connected setup.

202  
203 1.4 Connection of the microdroplet generation unit and microdroplet generation control unit  
204 (Figure 1 Part 4, Part 5)

205  
206 NOTE: This part is connected to the  $\mu$ DG transport unit (step 1.3)

207  
208 1.4.1 Connect the prepared  $\mu$ DG unit to the microdroplet transport unit by inserting the  $\mu$ DG  
209 head into the sample inlet end of the torch.

210  
211 1.4.2 Connect the power supply to the  $\mu$ DG control unit.

212  
213 NOTE: The setup described here consists of a commercially available  $\mu$ DG head and  $\mu$ DG power  
214 supply. Depending on  $\mu$ DG head used the setup must be adapted accordingly.

## 215 216 2. Quantification of droplet size

217  
218 2.1 Use a stroboscope light and a CCD camera (e.g., in an open configuration, see **Figure 1**  
219 size measurement configuration) for taking images of produced droplets by the  $\mu$ DG.



221 2.2 Calibrate the CCD camera by taking images of an object of known size in  $\mu\text{m}$  range (e.g.,  
 222 copper wire with a diameter of  $150\ \mu\text{m}$ ).  
 223

224 2.3 Take images of at least 1, 000 drops at the settings used for the experiment (see **Table**  
 225 **2**).  
 226

227 2.4 Use an appropriate graphical software program (see **Table of Materials**) to evaluate the  
 228 images concerning the object and drop size in the following steps:  
 229

230 2.4.1 Click **File** and **Open** to load the image of the object.  
 231

232 2.4.2 Click **Image | Adjust | Threshold** to define the area of the object by moving the scroll  
 233 bars.  
 234

235 2.4.3 Click **Apply** to apply the settings.  
 236

237 2.4.4 Click on the **Straight** segment button.  
 238

239 2.4.5 Click and hold the left mouse button to draw a line alongside the object.  
 240

241 2.4.6 Press **Ctrl + M** to measure the object size.  
 242

243 2.4.7 Measure the diameter of the object at 5 different points.  
 244

245 2.4.8 **Copy** and **Paste** the “Results” table in a spreadsheet software.  
 246

247 2.4.9 Calculate the arithmetic mean of the column “Length”.  
 248

249 2.4.10 Calculate the pixel aspect ratio (PAR): actual object size ( $\mu\text{m}$ )/mean object size in the  
 250 image (px).  
 251

252 2.4.11 Click **File | Import | Image Sequence** to import and load the images of the droplets.  
 253

254 2.4.12 Click **Rectangular** and mark the droplet of the first image.  
 255

256 2.4.13 Perform the right click on the mouse pad and choose **Duplicate** to separate the droplets  
 257 of the image sequence from the rest of the image.  
 258

259 2.4.14 Separate the droplets from the background as specified in step 2.4.2.  
 260

261 2.4.15 Click **Process | Binary | Erode** to remove reflections of light on the droplet surface.  
 262

263 2.4.16 Click **Process | Binary | Dilate** to reverse the “Erode” step.  
 264

2.4.17 Click **Analyze | Analyze Particles | Ok** to measure all droplets.

2.4.18 **Copy** and **Paste** the “Summary” or “Result” table into a spreadsheet software.

2.4.19 Calculate the arithmetic mean of the ferret diameter in px.

2.4.20. Use the PAR to transform the diameter in  $\mu\text{m}$ : ferret diameter in px/PAR.

NOTE: The size of the droplets formed by the  $\mu\text{DG}$  varies depending on the selected length and duration of the current pulse applied to the piezo element<sup>7</sup>.

### 3. Sample preparation

3.1 Prepare an ionic calibration solution of the analyte to be measured in the concentration range of 0.2 to 20  $\mu\text{g/L}$  in dilute acid (e.g., HCl (0.5 v/v), HNO<sub>3</sub> (3.5 v/v)).

3.2 Prepare an ionic solution for the one-point calibration in the concentration range between 1 and 10  $\mu\text{g/L}$  in dilute acid.

3.3 Prepare the NP standard suspensions according to the manufacturer's instructions or in-house protocols.

NOTE: Steps 3.3.1 – 3.3.4 explain the preparation of the NP standard suspensions considering Ag, Au, CeO<sub>2</sub> NPs as example.

3.3.1 Prepare 10 mL of 0.05  $\mu\text{g/L}$  AuNP solution for the PN and 1  $\mu\text{g/L}$  AuNP solution in ultrapure water for  $\mu\text{DG}$ . Vortex for 20 – 60 s before using.

3.3.2 Prepare 0.05  $\mu\text{g/L}$  AgNP solution for the PN and 2  $\mu\text{g/L}$  AgNP solution, both in ultrapure water, for  $\mu\text{DG}$ . Shake well for 20 – 60 s before using<sup>15</sup>.

3.3.3 Prepare CeO<sub>2</sub> NP solutions to be used as described previously for metal oxides<sup>16,17</sup>.

3.3.4 Prepare 0.05  $\mu\text{g/L}$  CeO<sub>2</sub> NP solution for the PN and 1  $\mu\text{g/L}$  solution for the  $\mu\text{DG}$ .

3.3.4.1 Weigh 25.6 mg/mL CeO<sub>2</sub> NP in a glass vessel of 15 mL – 20 mL total and add 10 mL of 0.05 (v/v) BSA solution prepared in ultrapure water.

3.3.4.2 Use a fingertip sonicator with a power of 7.35 W to homogenize the particle solution for 309 s.

### 4. Instrumental tuning and parameters

4.1 Make sure the MDG generator is turned off and connect the dual-inlet sample

introduction setup which was built in step 1 with the injector of the ICP-MS instrument with a clamp. Flush the inlet system for 5 – 10 min with the nebulizer gas (Ar) and the droplet transportation gas (He).

NOTE: The ICP-MS instrument has to be protected against the penetration of high levels of oxygen into the plasma room.

4.2 Turn off the droplet transportation gas (He) and start the ICP-MS system

4.3 Tune the instrument in the measurement mode which one wants to utilize using the instrument standard tuning solution that is specified by the manufacturer of the ICP-MS system.

NOTE: A standard tuning solution consist of, for example barium, cerium, indium, uranium, bismuth, cobalt, lithium (all 1 µg/L) in a mixture of 2.5% (v/v) nitric acid and 0.5% (v/v) hydrochloric acid.

4.4 Determination of the sample uptake rate of the PN.

4.4.1 Fill a vessel with 15 mL of water.

4.4.2 Weigh the vessel.

4.4.3 Connect the vessel to the tubing of the PN.

4.4.4 Start the peristaltic pump by click on the peristaltic pump start button in the instrument software.

4.4.5 Start a 5 min timer.

4.4.6 Remove the uptake line from the vessel exactly after 5 min. Weigh the vessel again.

4.4.7 Calculate the sample uptake rate (mL/min) using the formula: vessel weight before - vessel weight after / time duration.

4.5 Optimize instrumental parameters to improve analyte sensitivity if necessary, e.g., nebulizer gas flow rate, sampling depth, plasma power.

NOTE: See **Table 2** as an example of instrumental parameters that can be optimized in an ICP-MS system.

4.6 Adjust the He gas flow until a constant signal rate can be detected as a function of the drop formation rate.

(Place **Table 2** here)

## **5. Multi-mode measurement of nanoparticle samples**

### **5.1 Prepare the $\mu$ DG control unit**

5.1.1. Turn on the power supply switch of the  $\mu$ DG control unit.

5.1.2 Click **Start** on the first screen to start up the control unit.

5.1.3 Click **Global Settings** to choose the pulse mode to be used.

5.1.4 Click on the right graphical button at pulse mode to choose the triple pulse mode.

NOTE: The settings for the triple pulse mode are given in **Table 2**.

### **5.2 Prepare the $\mu$ DG unit**

5.2.1 Click **On/Off** to start the  $\mu$ DG.

5.2.2 Fill the sample vessel with the sample solution to be measured.

5.2.3 Connect the sample vessel to the  $\mu$ DG unit.

5.2.4 Using a 10 mL syringe to purge air through the vessel and the  $\mu$ DG unit.

5.2.5 Connect the syringe to the syringe port on the sample container vessel.

5.2.6 Push the syringe plunger until a constant liquid stream is observed coming out the  $\mu$ DG head.

5.2.7 Maintain the pressure for 10 s.

5.2.8 Remove the syringe.

5.2.9 Place the  $\mu$ DG unit into the focus zone of the CCD camera to observe the formed droplets.

5.2.10 Connect the CCD camera to a PC or laptop.

5.2.11 Start the CCD camera software to observe the formed droplets

5.2.12 Click **Start** to get a live view of the droplets.

5.2.13 Observe constant droplet formation.

5.2.14 Place the  $\mu$ DG head onto the inverted torch on the dual-inlet sample introduction system.

5.3 Validate both, the  $\mu$ DG unit and the PN for each element of interest by measuring repeated multi point-calibrations.

NOTE: For ICP-MS data acquisition, use the software associated with the instrument.

5.4 Determine the linear range of the multi-point calibration by importing the experimental data into a spreadsheet software.

5.4.1 Calculate the arithmetic mean of each calibration point.

5.4.2 Determine the intercept, slope and correlation coefficient.

NOTE: For sp-ICP-MS the correlation coefficient should be  $>0.99^{18}$ .

5.5 Choose a concentration within the linear range of the calibration curves for one-point calibrations later on.

5.6 Following the steps below for measurement and validation (by using reference materials like NIST 8012, NIST 8013 or NIST 8017 or similar) of the multi-mode nanomaterial quantification (**Figure 2**).

5.6.1 Select a nanoparticle and an ionic standard according to the analyte of interest.

5.6.2 Prepare the  $\mu$ DG unit according to 5.2 with an ionic standard solution.

5.6.3 Add a diluted acid solution (e.g., 0.5% v/v HCl) via the PN.

5.6.4 Start the measurement of the ICP-MS system in time resolved mode.

5.6.5 Click **On/Off** after 120 s to stop the  $\mu$ DG and exchange the dilute acid solution at the PN with the ionic standard.

5.6.6 After 330 s once again exchange the ionic standard at the PN with a dilute acid solution.

5.6.7 Meanwhile remove the  $\mu$ DG unit from the setup.

5.6.8 Exchange the sample vessel (glass vial) of the  $\mu$ DG unit with a vessel containing a diluted acid solution (e.g., 3.5%  $\text{HNO}_3$ ) in order to clean the  $\mu$ DG unit.

5.6.8.1 Fill a 10 mL syringe with air.

5.6.8.2. Connect the syringe to the injection port of the  $\mu$ DG unit and empty the syringe until a jet of liquid appears from the  $\mu$ DG head and maintain pressure for 30 s.

5.6.8.3. Prepare the  $\mu$ DG as specified in step 5.2 with the NP sample and attach the  $\mu$ DG unit back to the setup at 510 s.

5.6.9. Click **On/Off** after 810 s to stop the  $\mu$ DG.

5.6.10. Exchange the dilute acid solution at the PN with the NP sample and measure for another 300 s.

5.6.11. Stop the measurement after approx. 1,200 s.

5.6.12 Clean the  $\mu$ DG unit as specified in step 5.5.8.

(Place **Figure 2** here)

## 6. Data analysis

NOTE: To simplify all calculation steps, a corresponding spreadsheet was prepared (see **Supplementary File**).

6.1. Use a spreadsheet or software which can handle data frames to process the data and import the measured data. Paste the intensity values of the entire measurement in the spreadsheet software (included in the electronic supplement) in column A, the data will be visualized. Enter all necessary experimental parameters for calculation into the table “Input Parameter”.

6.2. Define the regions of interest (ROI) for  $\mu$ DG ionic (I), PN ionic (II),  $\mu$ DG NP (III) and PN NP (IV) by selecting the appropriate spreadsheet cells. Using the graph in the prepared sheet to define the boundaries of the ROIs and enter the values into the “Determination of the Region of Interest” table (cells C1:E7).

6.3. Copy and paste the each data set in a separate column. Press the button **Copy ROI** in the prepared sheet to split the measurement into the four ROIs (column M:P).

6.4. Calculate the arithmetic mean of I and II.

6.5. Apply the iterative approach to separate particle or droplet signals and background for III and IV.

6.5.1. Calculate the arithmetic mean and standard deviation of all measured values.

6.5.2. Calculate a limit or cut-off value by mean value + 5\*standard deviation.

6.5.3. Remove all signals smaller than the limit value of III and IV by using the **Cut** command on the identified particle signals. Use **Paste** to paste them in a separate column.

6.5.4. Repeat steps 1-3 until the mean value and standard deviation are constant.

NOTE: In columns Q to BD of the prepared sheet, the iterative approach to separate background and particle signals is performed five times.

6.6. Calculate the arithmetic mean of the identified particle signals of III and IV.

6.7. Calculate the minimum detectable particle size ( $LOD_{size}$  - nm) for  $\mu$ DG NP and PN NP by using the instrumental limit of detection of the analyte ( $LOD$  - counts), the analyte sensitivity ( $S_{C,ionic}$  - counts/( $\mu$ g/L)), the sample uptake rate ( $q_s$  - mL/min), the transport efficiency ( $\eta$  - relative unit) and the bulk material density ( $\rho$  - g/cm<sup>3</sup>):

$$LOD(counts) = I_{Background} + 5 * \sigma_{Background} \quad (1)$$

$$LOD_{size}(nm) = \sqrt[3]{\left(6 * \left(\frac{LOD}{S_{C,ionic}}\right) * \left(\frac{q_s}{60}\right) * \eta\right) / (\pi * \rho)} \quad (2)$$

6.8. Calculate the mass ( $m_{a,p}$ ) and particle size ( $d$  - nm, assuming the particles are spherical) of identified particle signals for  $\mu$ DG NP and PN NP according to the three analysis modes applied by taking the ionic metal concentration of a standard solution ( $c_a$  -  $\mu$ g/L) and the ion flux in the plasma (counts/s) into account:

$$6.8.1 \quad \text{Mass:} \quad m_{a,p}(fg) = \left(\frac{q_s * \eta * c_a}{q_{i,a}}\right) n_{i,p} * 10^{-6} \quad (3)$$

$$6.8.2 \quad \text{Size:} \quad d(nm) = \sqrt[3]{\frac{6 * m_{a,p}}{(\pi * \rho)}} \quad (4)$$

6.9 Calculate the specific transport efficiency of the analysis modes by using the number of particles detected ( $q_p$ ), the particle concentration of the sample ( $c_{p,used}$  - 1/mL), the analyte sensitivity of the PN and MDG ( $S_{m,ionic,PN}$ ,  $S_{m,ionic,MDG}$  - counts/( $\mu$ g/L)), the volume of the droplet ( $V_{drop}$  - pL), the dwell time ( $t_d$  - ms), the transport efficiency of the PN ( $\eta_{PN}$ ), the transport efficiency of the  $\mu$ DG ( $\eta_{\mu DG}$ ), the intensity of the ionic solutions measured by the PN and  $\mu$ DG ( $I_{ionic, PN}$ ,  $I_{ionic, \mu DG}$  - counts) and the concentration of the ionic solution used for both injection systems ( $C_{ionic,PN}$ ,  $C_{ionic, \mu DG}$  -  $\mu$ g/L) :

$$6.9.1 \quad \text{Mode I:} \quad \eta_{PN} = \frac{q_p}{c_{p,used} q_s} \quad (5)$$

6.9.2 Mode II: 
$$\eta_{PN} = \frac{S_{m,ionic,PN}}{S_{m,ionic,MDG}} = \left( \frac{S_{C,ionic,PN}}{S_{C,ionic,MDG}} \right) * \left( \frac{V_{Drop}}{q_s * t_d} \right) \quad (6)$$

$$S_{m,ionic,PN} \text{ (counts ng}^{-1}\text{)} = \frac{S_{C,ionic,PN}}{q_s * t_d * \eta_{PN}} \quad (7)$$

$$S_{m,ionic,\mu DG} \text{ (counts ng}^{-1}\text{)} = \frac{S_{C,ionic,\mu DG}}{V_{Drop} * \eta_{\mu DG}} \quad (8)$$

$$S_{C,ionic,PN} \text{ (counts (ng mL}^{-1}\text{))}^{-1} = \frac{I_{ionic,PN}}{c_{ionic,PN}} \quad (9)$$

$$S_{C,ionic,\mu DG} \text{ (counts (ng mL}^{-1}\text{))}^{-1} = \frac{I_{ionic,\mu DG}}{c_{ionic,\mu DG}} \quad (10)$$

6.10 Assume that the transport efficiency of  $\mu DG$  is equal to 1:<sup>19</sup>

$$\eta_{\mu DG} = 1 \quad (11)$$

6.11 Calculate the particle number concentration of the NP solution analyzed by taking into account the injected sample volume during the measurement ( $V_{injected}$ ):

$$c_{p,detected} \text{ (# mL}^{-1}\text{)} = \frac{q_p}{\eta} * \frac{1}{V_{injected}} \quad (12)$$

NOTE: In the prepared sheet all calculations are performed automatically after the splitting. The results are shown in table "Output Parameters" (cells BH7:BR35) and contains the formulas described above including individual calculation steps.

#### REPRESENTATIVE RESULTS:

(Place **Figure 3** here)

(Place **Figure 4** here)

(Place **Figure 5** here)

(Place **Table 3** here)

The protocol presented here allows for the determination of the particle mass and number concentration. The  $\mu DG$  droplet formation, including the droplet size (**Figure 3**) was characterized beforehand (**Table 3**).

After the setup was assembled (**Figure 1**) and the droplet size determined, both injection systems were validated with ionic standards (**Figure 4**). An accuracy of  $r^2 > 0.99$  could be achieved with both injection systems for all investigated elements. However, there are differences in both systems due to the amount of analyte introduced and transported. Since the  $\mu DG$  has a very high transport efficiency (up to 100%), higher analyte sensitivities compared to the PN are observed with low mass input at the same time. However, the measured concentrations introduced by the  $\mu DG$  have to be separated into two linear ranges. For Ag, the



first linear range can be observed between 0 and 0.5 fg event<sup>-1</sup> and the second between 0.5 and fg event<sup>-1</sup>. In contrast, the first linear range for Ce is between 0 and 0.25 fg event<sup>-1</sup> and the second between 0.25 and 3 fg event<sup>-1</sup>. The linear range for PN for the measured concentrations appears to be higher. This is most likely related to the difference of introduced mass into the ICP-MS per detection event. The  $\mu$ DG injects a constant absolute quantity in a low volume per drop and detection event resulting in lower detected mass compared to the introduction of samples with the PN.

After the successful validation, experiments can be performed as described in **Figure 2**. A result of such experiments is exemplified in **Figure 5** for the determination of the particle size and number concentration of CeO<sub>2</sub> NP. Here the signals for the introduced ionic and NP solutions via  $\mu$ DG and PN can be identified. A triple determination was carried out for all investigated particles.

The evaluation of the obtained data was performed as described above and is summarized in **Table 3**. For the Au and Ag NP used for validation of the dual-inlet setup and the three analysis modes, the certified particle size and number concentration could be achieved with all analysis modes performed. The mean particle sizes obtained for CeO<sub>2</sub> are between 10 and 100 nm, the range specified by the manufacturer.

#### FIGURE AND TABLE LEGENDS:

**Figure 1: Design of the dual-inlet interface setup.** Part 1 - connector unit, Part 2- conventional introduction system, Part 3 - microdroplet transport unit, Part 4- microdroplet generation unit, Part 5- microdroplet control unit, and open configuration for droplet size measurement including a stroboscope light and a CCD camera.

**Figure 2: Measurement strategy for multi-mode nanomaterial quantification.**

**Figure 3: Determination of the droplet size with the CCD-camera:** Calibration of the CCD-camera with a 150  $\mu$ m copper wire (A) and determination of the droplet size after converting the achieved droplet pictures into a binary color picture (B).

**Figure 4: Validation of the dual inlet-setup:** Multi-point calibration of the  $\mu$ DG (A) and PN (B) inlet system for gold (Au), silver (Ag) and cerium (Ce). The used concentration in the range of 0.2 – 20  $\mu$ g mL<sup>-1</sup> is converted, depending on used experimental conditions in mass per detected event. The presented data are the average values of three independent replicates.

**Figure 1: Representing measurement for the dual-inlet setup:** The quantification of CeO<sub>2</sub> NP with colored bars as done in Figure 2 for the different injection steps.

**Table 1: List of Components used to build up the dual-inlet setup.**

**Table 2: Values of instrumental parameters used.**

**Table 3: Results of the dual-inlet setup.** Transport efficiency, metal mass fraction, diameter and NP number concentration for Au NIST 8013, Ag NIST 8017 and CeO<sub>2</sub> JRC NM 212 (n=3) NP materials using three analysis modes and three transport efficiency determination methods. The % recovery is defined as the ratio of the determined #NPs to the expected #NPs. The table is reprinted with permission from reference<sup>14</sup>.

## DISCUSSION:

The aim of the developed dual-inlet setup is the characterization and quantification of NP as accurately as possible concerning their size and number concentration by using different analysis modes, independent of the analyte to be investigated. By combining a low volume (pL) and high mass transport (up to 100%) introduction system ( $\mu$ DG) with a conventional introduction system (PN) this is achievable. By using the setup presented in this work, the element-specific based transport efficiency required for quantification of particle mass can be determined based on ionic standards and independently of NP reference materials. In addition, the NPs introduced into the ICP-MS with the  $\mu$ DG have a narrower (AuNP) or similar (AgNP) particle size distribution. Otherwise, for CeO<sub>2</sub> a broader size distribution for the  $\mu$ DG was observed and can be attributed to the higher polydispersity of the analyzed sample. Due to the introduction of low volume two NPs can be detected separately from each other, which would otherwise be interpreted as one NP in the conventional setup<sup>14</sup>.

The advantages resulting from the  $\mu$ DG transport unit are the high degree of flexibility due to the flexible silicon tubing, which simplifies the alignment of the setup. The torch with the injector can also be adjusted during the setup while still connected to the ICP-MS. The additional applied He gas flow prevents a collision of the droplets formed by the  $\mu$ DG head with the tubing walls<sup>20</sup>. Furthermore, the He gas allows for the removal of  $\mu$ DG head during the sample exchange even when ICP-MS is still operating. Keeping the ICP in an operational state is crucial for stable and robust measurement. Since the  $\mu$ DG head must be cleaned and rinsed with every new sample or standard, the He flow is vital for the operation of the inlet system introduced in this work. Furthermore, all parts of the dual-inlet setup have to be correctly connected in order to prevent the penetration of oxygen into the system. In order to diminish oxygen in the presented setup, the system is flushed with the nebulizer and droplet transportation gas before the ignition of the plasma for at least 5 to 10 min.

When the formed droplets reach the connector unit, they are transported into the plasma by a nebulized liquid stream, also referred to as a wet-plasma condition. Compared to the use of dry plasma conditions this leads to an increased liquid content of the plasma. Consequently, the signal intensity decreases as well as fluctuation of the signal increase, i.e., a higher standard deviation of the mean measurement signal<sup>13</sup>. However, by using the  $\mu$ DG and concentrations in the range of 0.2  $\mu$ g/L signals above the background can be detected. The corresponding injected mass per droplet has low metal content, which is close to the detection limits for some elements (i.e., Au, Ag, Ce). If different concentrations for calibration along this limit are used two linear regions can be observed with an overlap at approximately 0.05  $\mu$ g/L for Ce and 2  $\mu$ g/L for Ag. Below the overlapping region the observed signals are close to the element specific

background<sup>21</sup>. Above these limit the linear working range of the  $\mu$ DG can be identified. Even with the ability to measure low concentrations, it is impossible to distinguish between ions and NP of the same analyte within a droplet if they are simultaneously present. Otherwise, by using the conventional introduction system the average ionic background can be determined and subtracted from all signals to get the particle signals only.

MDG based system also have several limitations which can be partially circumvented by the application of proposed dual inlet system. However, if the droplet frequency of  $\mu$ DG exceeds 50 Hz it is not possible to create a consistent droplet pattern. The formed droplets might collide and, therefore, exchange of analyte occurs. The correct adjustment of gas flow rates is also important for a reliable transport of the droplet into the ICP-MS system as well as for correct operation of the PN. The proposed dual inlet system currently does not support automation of the measurement procedure as there is a requirement of manually changing the sample solutions.

In future,  $\mu$ DG can be used for characterizing and quantifying NPs in complex matrices and environmental samples. To prevent clogging of  $\mu$ DG because of the higher solution viscosity, complexity, and surface tension, an appropriate head design should be used. Depending on the  $\mu$ DG head design and operation of the power supply, it might be possible to generate droplets that contain particle-like systems such as cells, micelles, or lipid carriers for which standard reference materials are not available at all.

#### ACKNOWLEDGMENTS:

This work was supported by BfR SFP 1322-642 for F.L.K and P.R., BfR SFP 1322-724 for D.R. and BfR senior scientist fellowship for S.A.P.

#### DISCLOSURES:

All authors declare no conflict of interest.

#### REFERENCES:

1. Linsinger, T. P. J., Peters, R., Weigel, S. International interlaboratory study for sizing and quantification of Ag nanoparticles in food simulants by single-particle ICPMS. *Analytical and Bioanalytical Chemistry*. **406** (16), 3835-3843 (2014).
2. Krystek, P. et al. Method development and inter-laboratory comparison about the determination of titanium from titanium dioxide nanoparticles in tissues by inductively coupled plasma mass spectrometry. *Analytical and Bioanalytical Chemistry*. **406** (16), 3853-3861 (2014).
3. Degueldre, C., Favarger, P. Y., Bitea, C. Zirconia colloid analysis by single particle inductively coupled plasma-mass spectrometry. *Analytica Chimica Acta*. **518** (1-2), 137-142 (2004).
4. Degueldre, C., Favarger, P. Y. Colloid analysis by single particle inductively coupled plasma-mass spectroscopy: a feasibility study. *Colloid Surface A*. **217** (1-3), 137-142 (2003).
5. Pace, H. E. et al. Determining transport efficiency for the purpose of counting and sizing nanoparticles via single particle inductively coupled plasma mass spectrometry. *Analytical Chemistry*. **83** (24), 9361-9369 (2011).

6. Verboket, P. E., Borovinskaya, O., Meyer, N., Gunther, D., Dittrich, P. S. A new microfluidics-based droplet dispenser for ICPMS. *Analytical Chemistry*. **86** (12), 6012-6018 (2014).
7. Shigeta, K. et al. Application of a micro-droplet generator for an ICP-sector field mass spectrometer - optimization and analytical characterization. *Journal of Analytical Atomic Spectrometry*. **28** (5), 646-656 (2013).
8. Gschwind, S., Hagendorfer, H., Frick, D. A., Gunther, D. Mass quantification of nanoparticles by single droplet calibration using inductively coupled plasma mass spectrometry. *Analytical Chemistry*. **85** (12), 5875-5883 (2013).
9. Gschwind, S. et al. Capabilities of inductively coupled plasma mass spectrometry for the detection of nanoparticles carried by monodisperse microdroplets. *Journal of Analytical Atomic Spectrometry*. **26** (6), 1166-1174 (2011).
10. F. Zarrln, S. L. K., J. R. Socha. Droplet size measurements of various nebulizers using differential electrical mobility particle sizer. *Journal of Aerosol Science*. **22**, 343-346 (1991).
11. Geertsen, V., Lemaitre, P., Tabarant, M., Chartier, F. Influence of design and operating parameters of pneumatic concentric nebulizer on micro-flow aerosol characteristics and ICP-MS analytical performances. *Journal of Analytical Atomic Spectrometry*. **27** (1), 146-158 (2012).
12. Mehrabi, K., Günther, D., Gundlach-Graham, A. Single-particle ICP-TOFMS with online microdroplet calibration for the simultaneous quantification of diverse nanoparticles in complex matrices. *Environmental Science. Nano*. **6**, 3349-3358 (2019).
13. Ramkorun-Schmidt, B., Pergantis, S. A., Esteban-Fernandez, D., Jakubowski, N., Gunther, D. Investigation of a combined microdroplet generator and pneumatic nebulization system for quantitative determination of metal-containing nanoparticles using ICPMS. *Analytical Chemistry*. **87** (17), 8687-8694 (2015).
14. Rosenkranz, D. et al. Improved validation for single particle ICP-MS analysis using a pneumatic nebulizer/microdroplet generator sample introduction system for multi-mode nanoparticle determination. *Analytica Chimica Acta*. **1099**, 16-25 (2020).
15. Report of investigation reference material. *National Institute of Standards and Technology*. Reference material 8017 (2015).
16. Tavares, A. M. et al. Genotoxicity evaluation of nanosized titanium dioxide, synthetic amorphous silica and multi-walled carbon nanotubes in human lymphocytes. *Toxicology In Vitro*. **28** (1), 60-69 (2014).
17. Au - Kaur, I. et al. Dispersion of Nanomaterials in Aqueous Media: Towards Protocol Optimization. *Journal of Visualized Experiments*. (130), e56074 (2017).
18. ISO/TS19590 Nanotechnologies — Size distribution and concentration of inorganic nanoparticles in aqueous media via single particle inductively coupled plasma mass spectrometry. 2017.
19. Shigeta, K. et al. Application of a micro-droplet generator for an ICP-sector field mass spectrometer – optimization and analytical characterization. *Journal of Analytical Atomic Spectrometry*. **28**, 646-656 (2013).
20. Koch, J. et al. Accelerated evaporation of microdroplets at ambient conditions for the on-line analysis of nanoparticles by inductively-coupled plasma mass spectrometry. *Journal of Analytical Atomic Spectrometry*. **28** (11), 1707-1717 (2013).
21. Tuoriniemi, J., Cornelis, G., Hasselov, M. A new peak recognition algorithm for

741 detection of ultra-small nano-particles by single particle ICP-MS using rapid time resolved data  
742 acquisition on a sector-field mass spectrometer. *Journal of Analytical Atomic Spectrometry*. **30**  
743 (8), 1723-1729 (2015).  
744

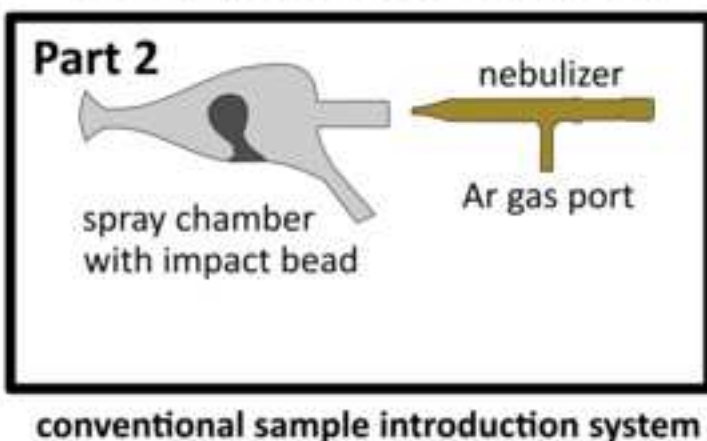
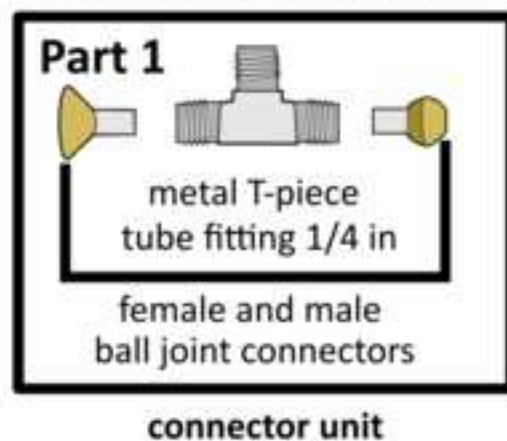
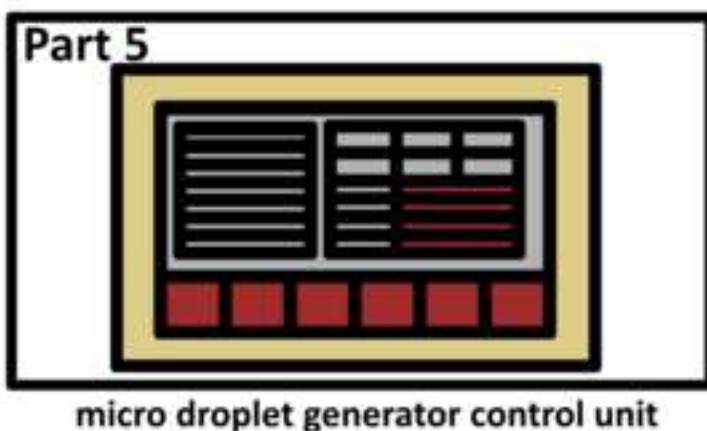
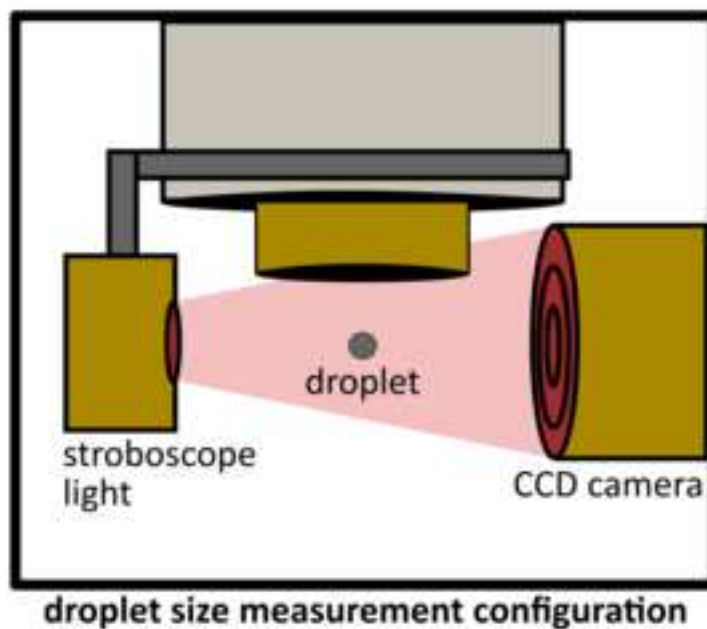
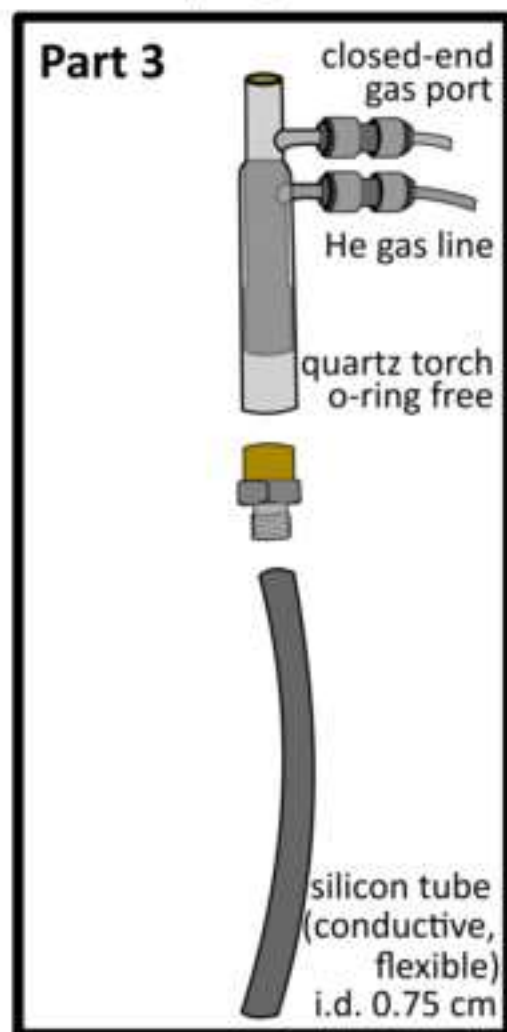
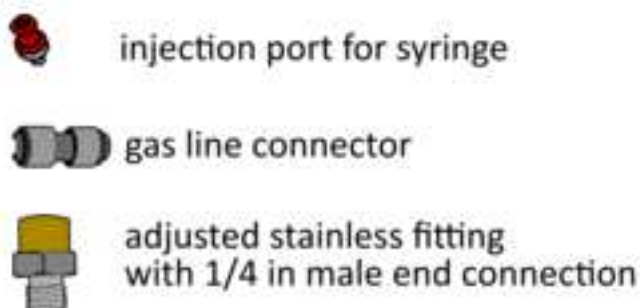
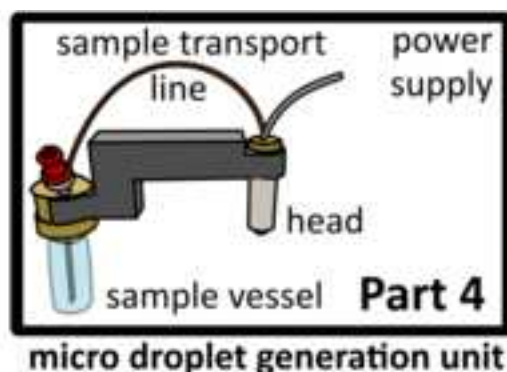
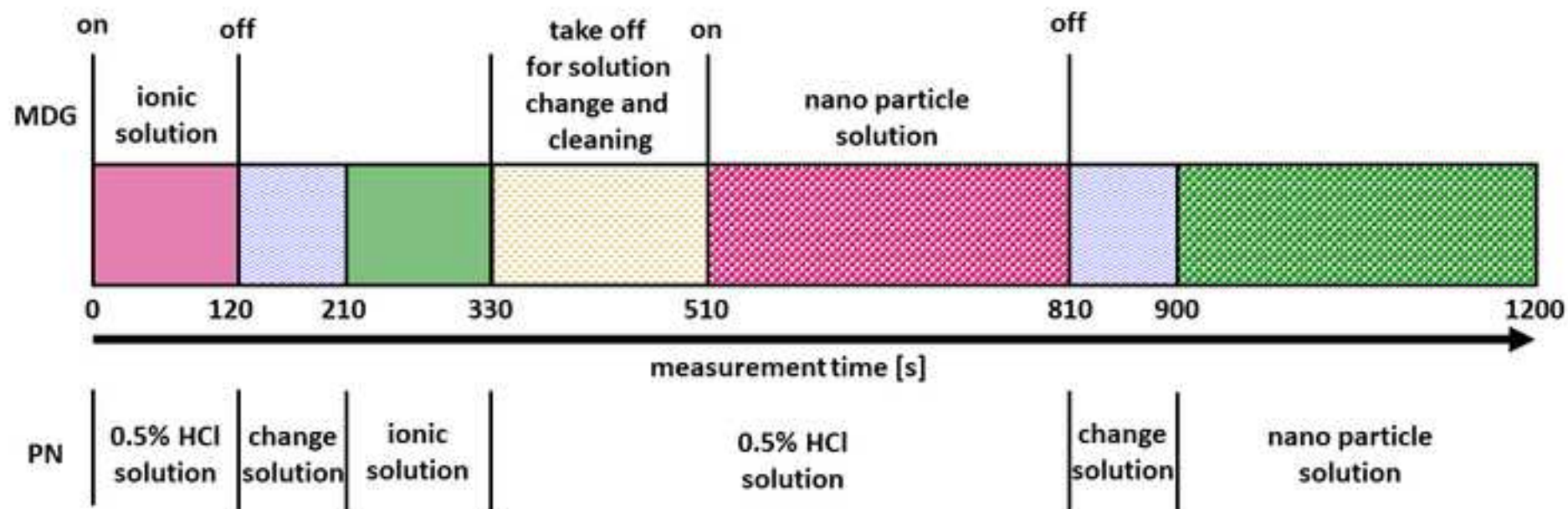
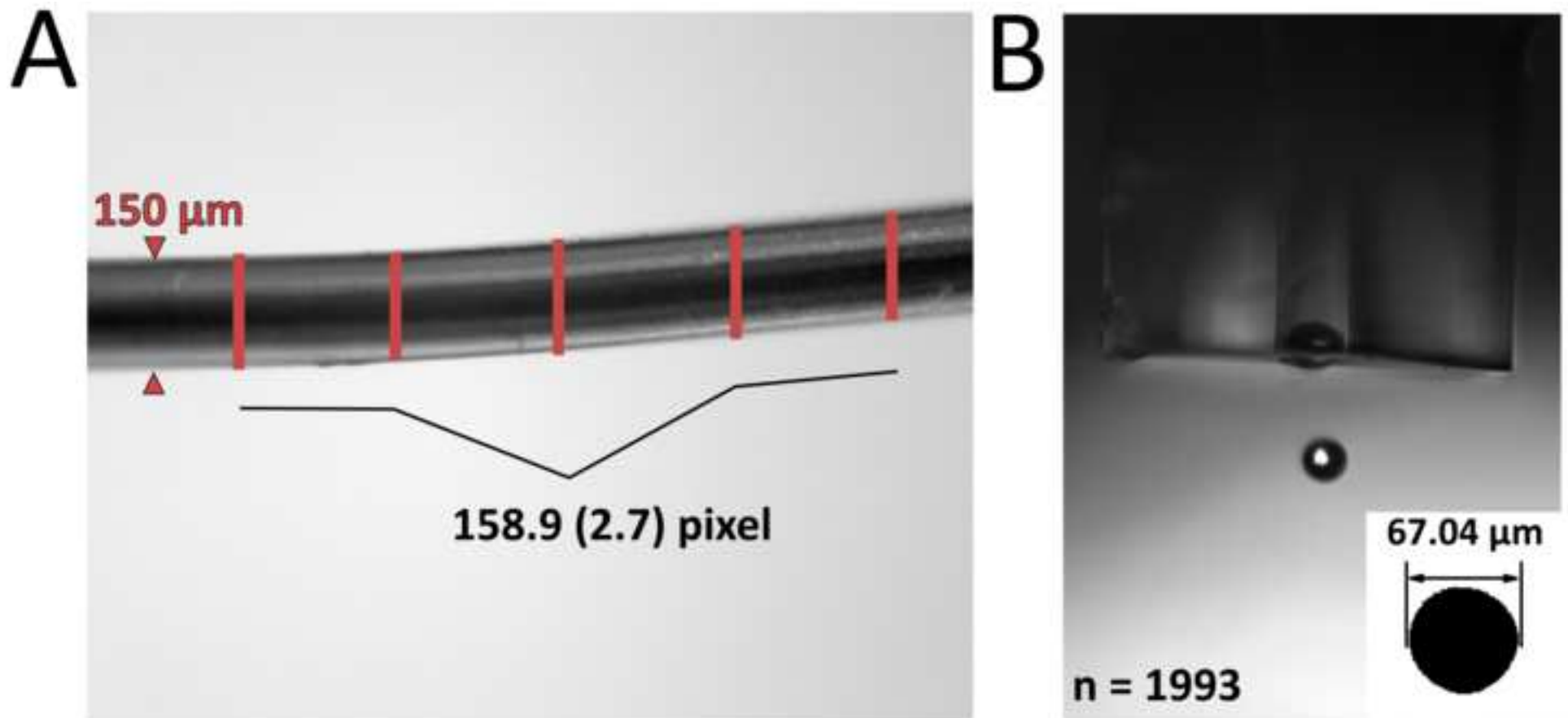


Figure 2







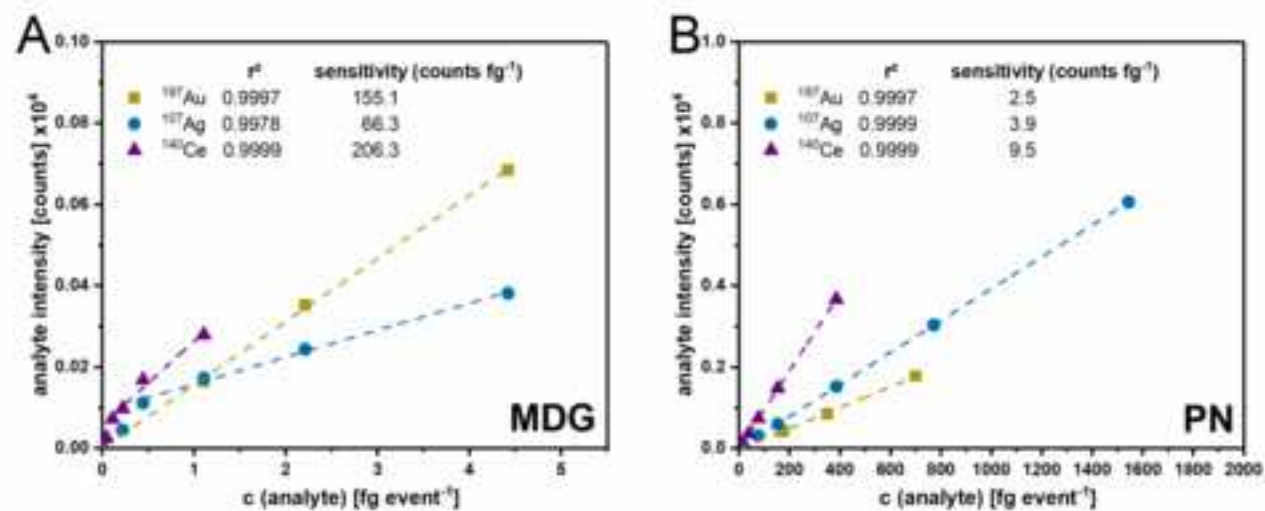
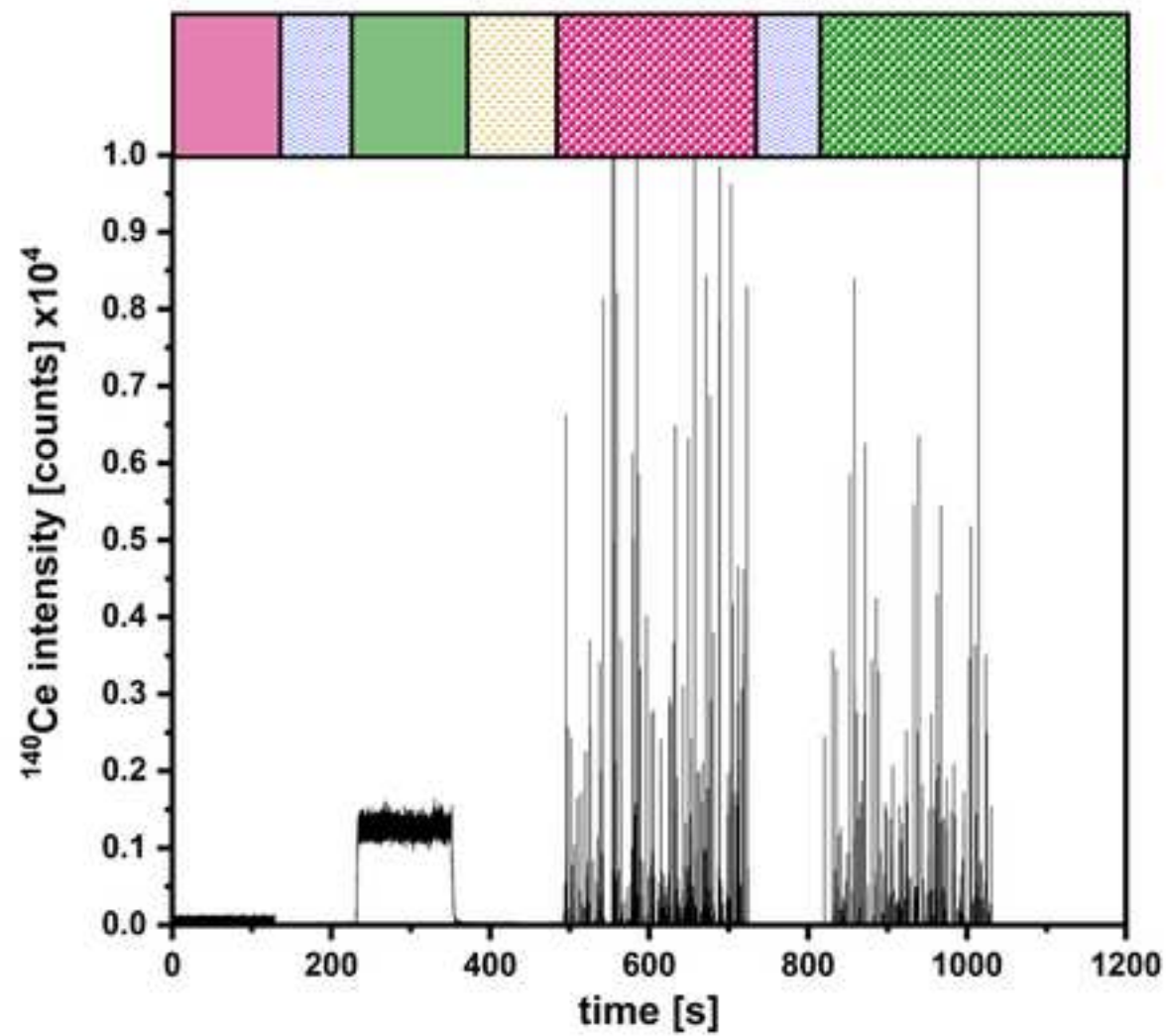


Figure 5



---

Part 1

---

Part 2

---

Part 3

---

Part 4

---

Part 5

---

## Components

---

Glass female spherical ball joint with approximately 10 mm shank length

Glass male ball joint with approximately 10 mm shank length

Metal T-piece (dimensions: 1/4 in)

Glass to metal adhesive

Two clamps for spherical glass joints

---

ICP-MS spray chamber (suggested type: impact bead spray chamber, cyclonic spray chamber or similar)

Pneumatic nebulizer (suggested type: concentric nebulizer)

Clamp

---

O-ring free quartz torch

Gas line connector closed-end

Gas line connector open-end

Conductive and flexible silicone tube

---

Piezoelectric Micro droplet generation unit

---

Micro droplet control unit

---

Parameter	Value		
<b>ICP – MS:</b>			
Plasma Power (W)	1600		
Sampling Depth (mm)	4		
Flow rates (L min <sup>-1</sup> ):			
Auxiliary Gas	0.65		
Cooling Gas	14		
Times (s)			
Data acquisition (s)	1200		
Dwell time (s)	0.01		
<b>Interface:</b>			
PN Sample uptake rate (mL min <sup>-1</sup> )	0.21		
Nebulizer Gas (L min <sup>-1</sup> )	0.92		
<b>μDG:</b>			
Capillary diameter (μm)	75		
Drop rate (Hz)	10		
He makeup gas (L min <sup>-1</sup> )	0.27		
Operation mode	Triple pulse		
	Set1	Set2	Set3
Voltage (V)	53	51	47
Pulse width (μs)	20	25	12
Pulse delay (μs)	4	2	1

Sample	Analysis Mode /		Inlet for NP sample	Inlet for calibration standards	$\eta$
	$\eta_{PN}$ determination				(%)
Au 56 nm NIST 8013	Mode-I / Counting Method		PN	PN: Au ionic & AuNP standards	1.8 (0.1)
	Mode-II / Sensitivity Ratio		PN	PN/ $\mu$ DG: Au ionic standards	1.9 (0.1)
	Mode-III / $\eta_{\mu DG} = 1$		$\mu$ DG	$\mu$ DG: Au ionic standard	100
	Expected size (nm)				
Ag 75 nm NIST 8017	Mode-I / Counting Method		PN	PN: Ag ionic & AgNP standards	2.3 (0.2)
	Mode-II / Sensitivity Ratio		PN	PN/ $\mu$ DG: Ag ionic standards	2.5 (0.2)
	Mode-III / $\eta_{\mu DG} = 1$		$\mu$ DG	$\mu$ DG: Ag ionic standard	100
	Expected size (nm)				
CeO <sub>2</sub> JRC NM212 10-100 nm	Mode-I / Counting Method		PN	PN: Ce ionic & AuNP standards	1.7 (0)
	Mode-II / Sensitivity Ratio		PN	PN/ $\mu$ DG: Ce ionic standards	4.9 (1.4)
	Mode-III / $\eta_{\mu DG} = 1$		$\mu$ DG	$\mu$ DG: Ce ionic standard	100
	Expected size (nm)				

$m_{a,p}$	NP size ( $d$ )	#NPs	Recovery
(fg)	(nm)	(mL <sup>-1</sup> x10 <sup>3</sup> )	(%)
1.9 (0.5)	57.2 (4.3)	28.1	100
		0	
2 (0.4)	58	25.6	91
	-3.6	-1.6	
1.7 (0.2)	55	394.4	70
	-2.4	-29.3	
	56.0 (0.5)		
1.9 (0.2)	70.2 (2.3)	21.6	100
		0	
2 (0.2)	71.5 (2.1)	20.5	95
		-1.9	
2.5 (0.2)	76.7 (2.3)	757.1	88
		-68.7	
	74.6 (3.8)		
0.90 (0.09)	61.9 (2.0)	7.59	-
		-0.32	
1.36 (0.35)	70.6 (5.9)	5.42	-
		-1.7	
1.63 (0.62)	74.4 (9.2)	590	-
		-168	

Name of Material/Equipment	Company	Catalog Number	Comments/Description
Au ionic (1000 mg L <sup>-1</sup> stock)	VWR, UK	85550.18E	
Ag ionic (1000 mg L <sup>-1</sup> stock)	Ultra Scientific, RI, USA	ICM-103	
Ag NP (75nm, NIST 8017)	NIST, Gaithersburg, MD, USA		no longer available
Au NP (60nm, NIST 8013)	NIST, Gaithersburg, MD, USA		no longer available
Ce ionic (1000 mg L <sup>-1</sup> stock)	VWR, UK	85557.18E	
CeO <sub>2</sub> (10-100nm, NM212)	EU Joint Research Centre	NM212	
Excel 2016	Microsoft		
Fiji	ImageJ		
Glass female spherical ball + Glass male ball	Fisher Scientific	12499016	
HCl (emprove bio)	Merck, Germany	100317	
ICP-MS spray chamber with impact bead	LabKings	LK6-45013 (OEM 3600170)	
Metal clamps for spherical glass joint	Fisher Scientific	11322015	
Metal T-Piece	Swagelok	SS-4-VCR-T	
Microdrop Dispenser Head, non heated	microdrop Technologies	944	
Microdrop Dispensing System MD-E-3000	microdrop Technologies		
MilliQ water (MilliPore gradient)	Merck MilliPore, Darmstadt, Germany		
O-ring free quartz torch	Analytical West Elemental	450-301	
PFA-ST concentric nebulizer	Scientific	ES-2042	
Silicone Rubber Tubing - 60° Shore - Platinum Cured - Black	Silex		
XIMEA Cam Tool	XIMEA		



**Reviewers' comments:****Reviewer #1:**

## Manuscript Summary:

The authors developed a dual-inlet setup for characterizing nanoparticles (NPs) by single particle inductively coupled plasma mass spectrometry (spICP-MS) without a reference NP standard. It consists of a pneumatic nebulizer (PN) for NP solutions and a microdroplet generator ( $\mu$ DG) for ionic calibration solutions. As a key part of the setup, they developed a new and flexible interface to facilitate the coupling of PN,  $\mu$ DG, and the ICP-MS system. They found that by using the setup, three independent analysis modes are available for determining the particle size and number concentration of NPs. The developed dual-inlet setup and its application will be of interest to researchers using spICP-MS techniques for analysis of NPs. However, the authors have not consistently reached the same results among the three modes and evaluated the robustness of the suggested setup. Please consider the following comments to improve the clarity and comprehensiveness of the manuscript.

## Major Concerns:

## Title

It is unclear where the terms "improved" and "robust" in the title come from and which data given in the text can support them. This reviewer believes that the terms should be corrected to be matched with the content of the text.

We thank the reviewer for his comment about the title of the submitted manuscript. Due to reviewers comment the title was changed into the following:

“Versatile dual-inlet sample introduction system for multi-mode single particle inductively coupled plasma mass spectrometry analysis and validation”

## Page 2, line 105

In conjunction with the above concern, how did the authors evaluate the robustness of the suggested setup? If they did not evaluate it, they cannot use the term "robust" here as well as in the title.

The title was changed according to the reviewer's comment, and we hope that our following explanation provides clarity. “Robust” is used to describe the ICP-MS stability and uninterrupted operational state, even during the time that the  $\mu$ DG is removed and therefore the inlet remains open. Removing the  $\mu$ DG does not cause plasma extinction, and the recorded ICP-MS signal is rapidly restored when the  $\mu$ DG is brought back to its operational position on the system. This “robust” system allows for rapid sample exchange as well as convenient  $\mu$ DG rinsing.

## Page 11, Eq. (6)

Why can the two factors " $\eta$ PN" and " $\eta$  $\mu$ DG" be cancelled during the transformation of the equation? It is not always true that their values are the same. This point should be clarified.

We thank the reviewer for his careful observation. An explanation of equation 6 was added at the end of section “6. Data Analysis” and we hope that it enhances the readability of the submitted manuscript:

The transport efficiency calculated by equation 6 assumes that  $\eta_{\mu\text{DG}}$  equals 1, as 100% of the analyte reaches the plasma through the  $\mu\text{DG}$  (as mentioned in ref 17, but also we observe the correct number of particles according to operating frequency of the  $\mu\text{DG}$ ). This in turn allows for determining the transport efficiency of the pneumatic nebulizer, with the only prerequisite of introducing a dissolved calibration standard through both inlets.

Page 13, Figure 4

Page 15, lines 415 and 416

In the case of the  $\mu\text{DG}$ , the linearity of the calibration curves for  $^{107}\text{Ag}$  and  $^{140}\text{Ce}$  was worse than that for  $^{197}\text{Au}$ . Regarding this trend, the authors mentioned later as follows.

"However, the measured concentrations introduced by the  $\mu\text{DG}$  have to be separated into two linear ranges."

If so, how can they explain that  $^{197}\text{Au}$  only exhibited the linear calibration curve with no separation? It seems to this reviewer that the  $\mu\text{DG}$  has unnoticed problems. In this context, the calculation of  $r^2$  values for three elements should be confirmed again whether correct or not, because the calibration curve for  $^{197}\text{Au}$  (with  $r^2$  of 0.9997) looks more linear than that for  $^{140}\text{Ce}$  (with  $r^2$  of 0.9999). These two points should be clarified.

For  $^{197}\text{Au}$ , ionic concentrations below  $5 \text{ ng mL}^{-1}$  were not tested, and this is probably the reason why the degree of linearity seems greater. We assume that the picture of the Au calibration curve for the low-end concentration range would be similar to the case of Ag and Ce, elements which were indeed tested for lower analyte concentrations. As mentioned in the paper (page 15 line 413 -415 of the original manuscript) the solution volume introduced by the  $\mu\text{DG}$  is by far lower compared to the PN (detecting fg of analyte per droplet compared to 1000s of fg in PN) and so an analyte concentration at the low  $\text{ng mL}^{-1}$  range (Ag range) cannot be distinguished clearly from a blank signal. Due to these points a direct comparison of the two introduction systems at the low  $\text{ng mL}^{-1}$  range is not possible (shown in the supplementary information of the original paper: <https://doi.org/10.1016/j.aca.2019.11.043>).

In order to address the remark of the reviewer and to clarify these points the following sentence was added into the discussion of the revised manuscript:

Below the overlapping region the observed signals are close to the element specific background. Above these limit the linear working range of the  $\mu\text{DG}$  can be identified.

Page 14, Table 6

Why were the recoveries of Au 56 nm and Ag 75 nm in the three analysis modes were so different each other? In the case of Au 56 nm, as a typical example, the difference in the recoveries obtained in Mode-I and Mode-III reached 30 %. In the both cases of Au 56 nm and Ag 75 nm, the difference in their recoveries obtained in Mode-I and Mode-II reached 5-9 %, although the transport efficiencies of the NPs were almost the same (i.e. ca. 2 %). Moreover, in the Excel file provided as an electronic supplementary material, the difference in the recoveries of Au 56 nm obtained in Mode-I and Mode-II amazingly reached 20 %. In addition to the above, why were the transport efficiencies of  $\text{CeO}_2$  JRC obtained in Mode-I and Mode-II different by 3.2 %? This difference is significantly larger than the cases of Au 56 nm and Ag 75 nm. These two points should be clarified.

We thank the reviewer for this interesting question about the recoveries with the different modes of analysis. We would like to state that small variations ( $c(\text{NP})$ ) in transport efficiency ( $\eta$ ) lead to a large variation in the particle number concentration. Attached below is an example, showing the effect of varying  $\eta\%$  to the  $c(\text{NP})$  determination.

The reason for which mode III exhibits a larger deviation in the determined  $c(\text{NP})$  compared to modes I and II could be attributed to the higher number concentration of particles injected through the  $\mu\text{DG}$ , leading to particle aggregation and therefore accounting for the lower recoveries.

$\text{CeO}_2$  JRC is a challenging material for spICP-MS analysis mainly due to its polydispersity and uncertainty in particle geometry. Granted that Mode I determines  $\eta$  by counting the number of particles detected, a possible particle aggregation could lead to a certain bias in the single particle events detected; meaning that signals coming from multiple particles could be counted as a single particle event.

For example: The following calculations are done by using equation 12 with  $q_p = 100$  NP detected,  $V_{\text{injected}} = 0.25$  mL, and the expected particle number concentration is  $22,500$  NP  $\text{mL}^{-1}$ . Please keep in mind that  $\eta$  is used as relative value in equation 12.

$\eta$ (%)	$C_{p,\text{detected}}$	Bias (%)
1.5	26667	18.52
1.7	23529	4.57
1.8	22222	-1.24
1.9	21053	-6.43
2	20000	-11.11
2.2	18182	-19.19

We hope this example answers the raised question sufficiently.

Minor Concerns:

Page 1, lines 43-46

Regarding the sentences below, which mode does "the third mode" indicate among the three modes given in the Page 11?

"While two analysis modes are known from the literature the third mode, introduced by this study, determines the transport efficiency using the data of inorganic ionic standard solutions. It is independent of reference materials."

It is unclear to this reviewer.

We thank the reviewer for spotting this misleading sentence. In order to clarify the named modes, the following sentences of Page 1 line 43 -46 was changed as follows:

While mode I (counting) and mode III ( $\mu\text{DG}$ ) are known in the literature, mode II (sensitivity), introduced by this study, is used to determine the transport efficiency by simply introducing ionic calibration standard via each mode and taking the sensitivity ratio obtained for each mode.

Page 1, lines 61 and 62

The sentence below is understandable to this review.

"The transport efficiency describes the ratio of the mass or particle number injected to the intensity values measured by the ICP-MS."

It should be corrected; otherwise additional explanation should be provided for that.

The mentioned sentence was corrected in order to enhance the readability of the revised manuscript:

The transport efficiency describes the ratio of the mass or particle number injected to the mass (waste collecting method) or particle number (counting method) detected by the ICP-MS.

Pace, H. E.; Rogers, N. J.; Jarolimek, C.; Coleman, V. A.; Higgins, C. P.; Ranville, J. F., Determining Transport Efficiency for the Purpose of Counting and Sizing Nanoparticles via Single Particle Inductively Coupled Plasma Mass Spectrometry. *Analytical Chemistry* **2011**, 83 (24), 9361-9369.

Page 1, line 67

There are some sources of the differences other than the "elemental composition" such as the structure and the dispersant as mentioned. Thus, this part should be corrected.

The reviewer correctly states other sources for the observed differences, we changed the mentioned section and thank the reviewer for his careful observation:

However, the transport properties depend on the structure of the NP, like the composition and the sample dispersant. Other influencing factors are instrumental parameters, like sample uptake rate, nebulizer gas flow rate, dwell time and total measurement time.

Page 1, lines 70-73

Appropriate references should be cited for the sentence below to clearly show the superiority of a  $\mu$ DG over a PN in terms of the probability of multi-particle events.

"It has been demonstrated that a continuous sample flow of PN increases the probability of multi-particle events, whereas injection of discrete sample volumes by a  $\mu$ DG (pL in a given time interval) lowers the probability of such events."

This reviewer believes that the probability of multi-particle events totally depends on the particle number concentration in the measured sample and therefore, a PN can work at the same level as  $\mu$ DG depending on the particle number concentration in the measured sample.

Unfortunately, the others of the manuscript were not able to find an appropriate reference that shows the superiority of a  $\mu$ DG over a PN in terms of the probability of multi-particle events.

The probability which was addressed within the sentence was related to the low volume injected by the  $\mu$ DG and is not based on Poisson statistics. In order to prevent confusion of the reader we decided to remove the mentioned sentence from the manuscript.

Page 1, line 75

What is the reason for "low injection volumes" being preferable? If there is a large amount of sample, small injection volume can lead to biased result.

We thank the reviewer for his question. The low injection volume is not only utilized to analyze higher particle number concentrations as for conventional injection systems. These low volume systems are also able, to detect particles which have a close proximity to each other, and to differentiate whether these particles are individual particles or have formed an agglomerate.

The sentence addressed by the reviewer was changed into following:

To be independent of reference materials, ideally, a sample introduction system with a transport efficiency of almost 100% is preferable. At the same time when a low volume is used compared to conventional introduction systems, there can be better distinguished between particles close to each other and higher particle number concentrations used.

Page 2, lines 85-89

Appropriate references should be cited for the sentence below to clearly show the superiority of a  $\mu$ DG over a PN in terms of the analyte sensitivity, etc.

"Due to the uniform sample introduction at high transport efficiency of 100% of the  $\mu$ DG, high instrument specific analyte sensitivity can be achieved. Depending on the matrix used, this leads to lower limits of detection (LOD) of particle mass and size when compared to the results of conventional introduction systems based on PN."

The missing reference was added:

Mehrabi, K., Günther, D., Gundlach-Graham, A., Single-particle ICP-TOFMS with online microdroplet calibration for the simultaneous quantification of diverse nanoparticles in complex matrices. *Environ. Sci.: Nano* **2019**, 6.

<https://doi.org/10.1039/C9EN00620F>

Page 3, Table 1

Regarding Part 2, why do the authors suggest these types of ICP-MS spray chambers and PNs? The reason for that should be mentioned somewhere because it could be informative.

We thank the reviewer for raising this issue. In fact, we have only experience for the available spray chambers, which are used in our lab. We also found, no other combinations with  $\mu$ DG in the literature. Irrespective of this other spray chambers can be attached to the shown setup.

In order to address the question a note was added to Table 1 Part 2:

Instead of the impact bead spray chamber other spray chambers with transport efficiencies typically in range of 2 to 10 % or higher can be used.

Page 7, line 236

What is the procedure below based on?

"Vortex or shake each solution for no more than 10 s."

In the nanoComposix protocol, for example, a longer time than 10 s is acceptable as follows.

"During storage, the nanoparticles may settle to the bottom of the vial (especially nanoparticles > 30 nm in diameter). Prior to aliquoting or use, resuspend the settled nanoparticles by vigorously shaking the bottle until the solution is homogenous. This will typically require ~30 seconds of mixing. ..."

Thus, appropriate references should be cited here to show the validity of the procedure.

We thank the reviewer for raising this point. The sample preparation was done in according to the manufacturer specifications. For AuNP NIST 8013 30 seconds of vortexing and for AgNP NIST 8017 30 seconds of shaking was used. The mentions 10 s was a typing error and corrected:

Vortex (NIST 8013) or shake (NIST 8017) each solution for 20 - 60s.

The investigation report for NIST 8017 was cited according to the reviewers suggestion: Small, A. J., Watters, R. L., National Institute of Standards and Technology. *Report of Investigation Reference Material 8017*; 2015.

Page 7, line 238

What the value "approx. 2.56 mg mL<sup>-1</sup>" indicate? It is unclear to this reviewer.

The concentration 2.56 mg mL<sup>-1</sup> of nano particles in BSA based solution was derived from the NanoGenoTox protocol. Slightly deviation from this value are acceptable to achieve a stable particle dispersion.

Page 8, Table 4

Why did the authors set the sampling depth (i.e. sampling position from the load coil) to 4 mm? This is far away from the normal sampling depth in the 8-10 mm range. The reason for that should be mentioned somewhere.

The sampling depth was optimized to reach the highest possible sensitivity for gold with the developed dual-inlet setup. The sampling depth was listed as the parameter used with our instrument iCAP Q from Thermo Scientific. For other instruments or analytes, the sampling depth can be different. To clarify, that the sampling depth can be optimized point 4.5 (in corrected manuscript) on page 7 was changed to:

Optimize instrumental parameters to improve analyte sensitivity if necessary, e.g. nebulizer gas flow rate, sampling depth, plasma power.

Page 9, lines 279 and 287

It seems strange to this reviewer that the sentence "Start the  $\mu$ DG" appears twice in one sequence of the  $\mu$ DG preparation without stopping it once. For clarifying that, the sentence

"Stop the  $\mu$ DG" should be inserted between them.

To overcome the addressed problem, point 5.4.4 was changes as follows: Start the measurement of the  $\mu$ DG.

When the  $\mu$ DG is prepared (5.1), it is started in the 1<sup>st</sup> step of  $\mu$ DG preparation (5.1.1).

Page 10, line 341

Is the term "larger" correct? It would be "smaller."

The reviewer's comment is correct, smaller signals indicated as background are removed from entire data set. As the reviewer suggested "larger" was exchanged by "smaller".

Page 11, line 353 and Eq. (11)

The authors only defined (or assumed) that the factor " $\eta\mu$ DG" is 1; in other words, they did not calculate it. Thus, the previous phrase (given below) looks strange to this reviewer.

"Calculate the specific transport efficiency of the analysis modes:"

It should be changed to be correct.

In order to address this question we would like to highlight, that the transport efficiency of the  $\mu$ DG is 1 because a particle enters the plasma and is detected by the ICP-MS according to the operation frequency of the  $\mu$ DG, which means there are no missing particles. If one assumes that the  $\mu$ DG device is set to 10 Hz and 10 signals per seconds are detected via ICP-MS than naturally the  $\eta_{\mu$ DG is 1.

The transport efficiency for the  $\mu$ DG is not calculated, it is only assumed to be 1 (relative) based on literature. Therefore, the calculation part for the  $\mu$ DG in the revised manuscript was changed as follows:

Assume that the transport efficiency of Mode III is equal to 1:<sup>17</sup>

Page 11, Table 5

The two factors " $n_{i,p}$ " and " $t_d$ " should also be defined here in this table.

We thank the reviewer for spotting the missing factors. We added the missing factors into table 5.

Page 16, lines 467 and 468

The sentence below is not true based on the Table 6.

"In addition, the NPs introduced into the ICP-MS with the  $\mu$ DG have a narrower particle size distribution."

In the case of CeO<sub>2</sub> JRC, for example, the standard deviation of the mean for the NP size obtained by Mode-III using the PN is larger than that obtained by Mode-I using the  $\mu$ DG.

Thus, the sentence should be corrected.

To clarify the difference of the observed size distributions a more detailed explanation was added:

In addition, the NPs introduced into the ICP-MS with the  $\mu$ DG have a narrower (AuNP) or similar (AgNP) particle size distribution. In contrast for CeO<sub>2</sub> a broader size distribution for the  $\mu$ DG was observed and can be attributed to the higher polydispersity of the analyzed sample.

Page 16, legend for Table 6

Since the reference #15 cited in the legend is the same as the reference #13, it should be cited correctly as the reference #13.

The doubling of reference 13 (now 14) was changed.

**Reviewer #2:**

In "Improved dual-inlet system for robust multi-mode single particle ICP-MS validation," the authors present a strategy for calibration of nanoparticle number concentration and nanoparticle mass distribution using only microdroplet based element standard solutions and nebulized element standard solutions. In my opinion, the biggest contribution of the authors with this manuscript is the modification of the dual-inlet setup by the use of conductive silicon tubing and modification of the ICP torch to accommodate a microdroplet dispenser head. In addition, the current manuscript provides a means for other practitioners of ICP-MS to build their own dual-inlet system; this is also a valuable contribution. However, before publication of this video manuscript, I think that several points should be addressed, which I've listed below:

\* In the abstract, and at several points in the manuscript, the authors claim that a "third analysis mode" is used to determine transport efficiency based on sensitivities obtained from the same element introduced in both droplets and with the pneumatic nebulizer. However, this analysis mode is actually "Mode II" in the manuscript. Calling this analysis mode the "third mode" and "Mode II" is confusing and should be fixed. Also, the claim that this Mode II transport efficiency calibration strategy is introduced in this manuscript is false. While, it is true that the authors published this work in Rosenkranz, D. et. al. Anal. Chim. Acta 2020, 1099, 16-25, a variation of this calibration strategy was actually already published before the manuscript by Rosenkranz et. al. under the name "online microdroplet calibration": Mehrabi, K.; Günther, D.; Gundlach-Graham, A., Environ. Sci.: Nano 2019, 6 (11), 3349-3358. K. Mehrabi also presented this calibration strategy in a poster at the European Winter Plasma Conference in 2019 in Pau, France. Appropriate citations should be added.

The mentioned part into the abstract was fixed:

While mode I (counting) and mode III ( $\mu$ DG) are known from the literature mode II (sensitivity), is used to determine the transport efficiency by inorganic ionic standard solutions only



The second citation was used in line 105 page 1.

\* The authors claim that "injection of discrete sample volumes by a  $\mu$ DG ... lowers the probability of [muliti-particle events]." This is, in principle, not true. It could be true that higher NP concentrations can be run with a  $\mu$ DG and still just get one particle per droplet; however, if a correct NP concentration is run via the pneumatic nebulizer, one also has low chances of coincident particle events. Moreover, with a pneumatic nebulizer, the sample is introduced continuously, so, if microsecond time resolved ICPMS analysis is made, one could even separate multi-NP events based on the shape of the measured time-resolved signals.

We thank the reviewer for his explanation and we are agreeing. To be correct, the addressed sentence was deleted.

\* In many microdroplet sample instruction setups, the microdroplet is viewed (and sized) online instead of prior to the placement of the  $\mu$ DG in its holder. In my experience, moving the  $\mu$ DG can lead to droplet instability, either in the form of a change in dispensed droplet size or in loss of the droplet. The authors should comment on challenges associated with removing and replacing the  $\mu$ DG so often in their workflow.

We thank the reviewer for raising this point. The  $\mu$ DG head is removed from the setup and after the sample solutions of the  $\mu$ DG are changed the  $\mu$ DG is placed carefully back to the setup while already running. Every time, when the  $\mu$ DG head was installed again into the setup signals were observed resulting from droplets. The variation into droplet size are not taking into account until now, because of the strong signal fluctuation depending on the wet-plasma conditions used.

\* In the section on LODs with microdroplets there is a mistake. The LOD for a microdroplet analysis of NPs must take into account the intensity and standard deviation of elemental signals from droplets that have no NPs in them, not the background in which droplet signals are not present. This should be corrected.

In order to correct this issue a more detailed description was added as note in line 364 page 11

To determine the background intensity in point 6.3 of the  $\mu$ DG the droplet signals which contains no particles should be used.

\* In figure 4, for the  $\mu$ DG calibration curve, the curve for silver is shallower than that for gold, but a higher sensitivity is reported for Ag107 than Au197. This is sloppy and inappropriate for publication. Also, in these plots, counts are plotted versus fg, but then the sensitivity is reported as cps/fg. Again, this makes no sense. Care should be taken in re-constructing these figures. Also, I do not know why droplet signals wouldn't produce entirely linear calibration curves. In the past, other authors have shown good linearity for microdroplet signals. Perhaps contamination is the reason for non-linear calibration? This should be better explained.

Figure 4 was checked ,redrawn and reanalyzed for mass per event injected according to the reviewers suggestion.

5

14201-

\* Citation 13 and 15 are identical. Please correct.

The citations were corrected.

### **Reviewer #3:**

#### **Manuscript Summary:**

This manuscript provides a detail procedure for nanoparticle measurement using a dual-inlet system. The authors presents most of the key steps to operate this correctly. It can be accepted after some minor revision.

#### **Major Concerns:**

1. uDG, Is it neccessary to be turned on the He gas of the head ? please emphasize this.

There was no possibility to use He gas on the  $\mu$ DG head directly. We know such a head is commercially available. The He was applied via the ICP-MS torch. By removing the  $\mu$ DG head from the setup the He gas reduce the entrance of oxygen into the setup. By removing the  $\mu$ DG head the setup is now opened and He gas can also leave through this opening against the flow direction of air.

An explanation why the He gas has to be used can be found in the revised manuscript at the protocol section (1. Assembly of the Dual-inlet sample introduction setup, 3<sup>rd</sup> point of Notes)

2. Figure 4, please give some explanation of why the signal response of Ag and Ce is not linear at the low concentration?

Because the lower concentrations are too close to the background, i.e. they cannot be fully separated from the background. As a result, ions getting lost and the observed signal intensity is reduced. The linear working range has to be defined when the used calibration point can be separated from the background.

In the manuscript the following sentence was improved:

If different concentrations for calibration along this limit are used two linear regions can be observed with an overlap at approximately  $0.5 \text{ ng mL}^{-1}$  for Ce and  $2 \text{ ng mL}^{-1}$  for Ag. Below the overlapping region the observed signals are close to the element specific background. Above these limit the linear working range of the  $\mu$ DG can be identified.

3. Figure 6, I suggest to provide some icons that mark the steps according to Figure 2

Figure 6 was changed to select the steps in according to figure 2

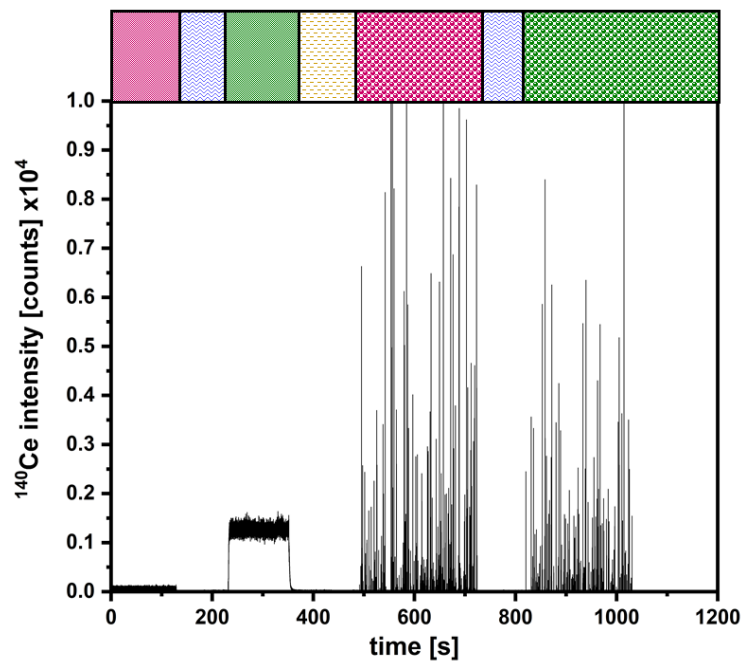


Figure 1: Representing measurement for the quantification of  $\text{CeO}_2$  NP with the dual-inlet system with colored bars in according to figure 2 for the different injection steps.

Request:

**Submission ID:** 986499

Date: 06 Mar 2020 1:45pm

Dear MSc Rosenkranz,

Thank you for submitting the Permission request form at <https://www.elsevier.com/authors/permission-request-form>. The following data have been recorded:

**Name:** MSc Daniel Rosenkranz

Institute/company: German Federal Institute for Risk Assessment (BfR)

Address: Max-Dohrn-Straße 8-10

Post/Zip Code: 10589

City: Berlin

State/Territory:

Country: Germany

Telephone:

Email: daniel.rosenkranz@bfr.bund.de

**Type of Publication:** Journal

Title: Analytica Chimica Acta

Auhtors: Daniel Rosenkranz, Fabian L. Kriegel, Emmanouil Mavrakakis, Spiros A. Pergantis, Philipp Reichardt, Jutta Tentschert, Norbert Jakubowski, Peter Laux, Ulrich Panne, Andreas Luch

Year: 2020

From page: 16

To page: 25

ISSN: 0003-2670

Volume: 1099

Article title: Improved Validation for Single Particle ICP-MS Analysis Using a Pneumatic Nebulizer / Microdroplet Generator Sample Introduction System for Multi-mode Nanoparticle Determination

**I would like to use:** Table(s)

Quantity of material: Table 1

I am the author of the Elsevier material: Yes

In what format will you use the material: Electronic

Translation: No

**Proposed use:** Reuse in a journal/magazine

Publisher of new work: jove

Title of new work: Improved dual-inlet system for robust multi-mode single particle ICP-MS validation

Authors of new work: Daniel Rosenkranz<sup>1</sup>, Fabian L. Kriegel, Emmanouil Mavrakakis, Spiros A.

Pergantis, Philipp Reichardt, Jutta Tentschert, Norbert Jakubowski, Peter Laux, Ulrich Panne, Andreas Luch

Answer:

Dear Daniel Rosenkranz

Thank you for your email.

- Please note that, as one of the Authors of this article, you retain the right for **re-using portions or excerpts in other works**

You do not require formal permission to do so. However suitable acknowledgement to the source must be made, either as a footnote or in a reference list at the end of your publication.

For full details of your rights as a Journal Author, please visit:

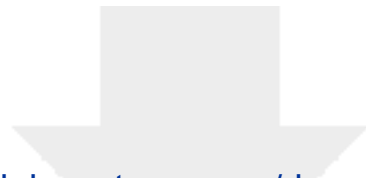
<https://www.elsevier.com/about/policies/copyright#Author-rights>

Please feel free to contact me if you have any queries.

Kind regards

**Anita Mercy**

Senior Copyrights Coordinator – Copyrights Team



[Click here to access/download](#)

**Supplemental Coding Files**  
Jove-MDG calculation sheets.xlsm

